

Topographic effects in strong ground motion



M. Rai, A. Rodriguez Marek

Virginia Polytechnic Institute and State University, United States

A. Yong

United States Geological Survey, United States

15 WCEE

LISBOA 2012

SUMMARY:

The influences of topography on site response are not considered in current ground motion prediction models. To begin analyzing the significance of these effects, we investigate geometric parameters that quantify surface topography to account for topographic effects when developing ground motion prediction equations (GMPEs). In this study, we test two topographic classification schemes: the first classification scheme is based on relative elevation information to categorize stations as sited either in high-lying, low-lying or neutral regions; whereas, the second scheme is a terrain-based classification approach developed by Iwahashi and Pike (2007). For each of these schemes, statistical tests are performed to check if the mean ground motion residuals in each classification group are significantly different. Preliminary results indicate that the mean ground motion residuals are different at long oscillator periods for high- and low-lying station classes using the relative elevation-based approach. Early results based on the terrain-based scheme, however, remain inconclusive.

Keywords: *Earthquake, strong ground motion, topography, terrain classification*

1. INTRODUCTION

Topographic (geometry) features such as hills, valleys and ridges have long been known to affect seismic ground motions (Bouchon, 1973; Boore *et al.*, 1981; Bard, 1982; Sánchez-Sesma, 1983; Geli *et al.*, 1988) and numerous case histories in the literature highlight this important effect (Çelebi, 1991; Spudich *et al.*, 1996; Assimaki and Gazetas, 2004; Grazier, 2009; Hough *et al.*, 2011). A notable example is the amplification of ground motion on top of a small hill in Tarzana during the 1994 M_w 6.7 Northridge earthquake. Most of the sites around the Tarzana location recorded peak ground acceleration (PGA) of 0.8 to 0.9 g; however, the acceleration on top of the flat, broad hill was recorded at 1.8 g (Shakal *et al.*, 1994). Although these observations were well documented and studied (Spudich *et al.*, 1996; Grazier, 2009), they are still not well understood hence are not typically considered in engineering design codes or in ground motion prediction equations (GMPEs) used for seismic hazard assessment and performance-based design. Topography-induced site amplification has the potential to affect design loads for buildings constructed on hills or valleys. Moreover, an improper characterization of topographic effects can also adversely impact estimates from the GMPEs. It is thus important to study these effects and include them in the predictive models. In this paper, we initiate a study about the effect of topography on ground motion by statistically analyzing recordings from a California strong motion database against various topographic parameters.

Our ground motion recordings are based on the California Small to Medium Magnitude (SMM) earthquake database compiled by Chiou *et al.* (2010). The SMM earthquake database consists of 188 earthquakes with magnitudes ranging from 3 to 5 for which the sole data source is the ShakeMap of California. The recordings were taken across 802 stations where 56 earthquakes were recorded within the northern California ShakeMap region and 132 earthquakes are within the southern California ShakeMap region. Chiou *et al.* (2010) analyzed this strong ground motion data to obtain a ground motion model for SMM earthquakes. Site effects were modeled using two parameters: the time-

averaged shear-wave velocity over the upper 30 meters (V_{S30}) and depth-to-one-kilometer-per-second ($Z_{1.0}$). We use the intra-event residuals (or within-event residuals) provided by Chiou *et al.* (2010). These residuals are the ground motion residual component that remains after accounting for earthquake-to-earthquake variability. If there is any bias in ground motion due to topography, the bias is expected to be present in this component.

Two approaches are used to assess the effects of topography on ground motions. In the first approach, topography is parameterized using a simple model where elevation information based on one arcsec (approximately 30-m grid spacing or pixel size) digital elevation models (DEMs) are used to classify stations as located in high-lying, low-lying or neutral regions. Researchers in the past have typically relied on spatial scale as a factor in topographic studies (Dikau *et al.*, 1991; Wood, 1996; Miliaresis and Argialas, 1999; Schmidt, 2004; Iwahashi and Pike, 2007). The second scheme is a globally consistent terrain-based classification method developed by Iwahashi and Pike (2007). Based on 30 arcsec (approximately 1-km grid spacing) Shuttle Radar Topography Mission DEMs, their approach relied on an unsupervised algorithm that divided the topography into 16 terrain classes as defined by slope gradient, local convexity and surface texture. The framework developed by Iwahashi and Pike (2007) was also the basis of a V_{S30} model developed by Yong *et al.*, (2012) to systematically account for site conditions (material composition). For each scheme, the analysis of variance (ANOVA) method is used to check if the means of each group within the classification schemes are significantly different.

2. DATA COLLECTION AND PROCESSING

To categorize stations in the elevation-based approach, one arcsec DEMs for California are downloaded from the USGS seamless server (<http://seamless.usgs.gov/index.php>). The downloaded data is obtained as individual grids (ArcGrid) in raster format where the native coordinate system is pre-assigned as North American Datum 1983 (NAD83). The mosaic function in the ArcGIS program is first used to combine all the rasters into one single raster layer; then, to analyze the data in units of meter, the layer is projected from NAD83 (in degrees of latitude and longitude) to the Universal Transverse Mercator coordinate system (UTM zone 10N).

The Iwahashi and Pike (2007) terrain classification model—also in the ArcGrid format—is readily downloadable from the Geospatial Information Authority of Japan webpage (http://gisstar.gsi.go.jp/terrain/front_page.htm). For California, we choose the America-centered (central meridian of 80W) GIS data option pre-assigned to the Robinson projection system and WGS84 datum. To associate the locations of the strong motion station sites to terrain classes, the list of station sites is first assigned to the World Geodetic Survey 1984 (WGS84) coordinate system and datum before reassignment to the Robinson projection system and WGS84 datum. These assignments are necessary because each layer in ArcGIS must be predefined into the same projection/coordination system and datum when spatial mathematics will be applied. Next, the list of strong motion station sites and terrain classification map are converted from text file and raster formats (respectively) to vector-based layers. The ArcGIS spatial-join function (nearest-neighbor option) is then applied on both layer-based data sets and a resultant table describing the relations between the strong motion station sites and terrain classes is produced.

The mosaicked raster and table are subsequently exported as text files for further analysis in the R statistical software package (R Development Core Team 2010).

3. ANALYSIS

3.1 Elevation-based classification

The following four parameters are used to classify a station location as high-, low- or neutral-lying:

- absolute elevation at the station
- scale (window size) representing the area considered
- mean elevation of area around the station
- threshold

The mean elevation is simply the average elevation in the area surrounding the station site. To define area, we use the term ‘scale’ to refer to the diameter of the circular region over which mean elevation is calculated. For our analyses, we rely on 12 different scales ranging from 250 to 3000 m at increments of 250 m. We classify each site as *high-lying* if the station elevation is higher than the mean elevation plus a threshold, and as *low-lying* if the station elevation is lower than the mean elevation minus a threshold. If the station lies in between these two values, we classify the site as *neutral-lying*. Thresholds of 10, 15, 20 and 25 meters are considered for each scale.

Each station in the SMM earthquake database had ground-motion recordings from one or more events (Chiou *et al.*, 2010). In order to account for bias due to sampling, we select only 412 stations that recorded at least 5 earthquakes and investigate the intra-event residuals for spectral acceleration (S_a) at periods of 0.01 s, 0.3 s and 1 s as well as residuals for peak ground velocity (PGV). Records for S_a at 3 s were not included because of poor data quality from analyses of signal-to-noise ratios (B. Chiou, personal comm., 2011). We then calculate the average residuals of S_a and PGV at each station where it is hereafter referred to as $\delta S2S_S$ (using the notation of Al Atik *et al.*, 2010) or the mean station within-event residual. Once we classify the stations into one of the three categories, we compute the mean $\delta S2S_S$ for all the stations within each group. Similarly, to calculate the standard deviation of intra-event residuals (ϕ), we compute the mean and the variance of the residuals at each site and then apply the law of total variance (Benjamin and Cornell, 1970):

$$\phi^2 = E(\phi_{ss,s}^2) + \text{Var}(\delta S2S_S) \quad (5.1)$$

where $\phi_{ss,s}^2$ is the variance of the intra-event residual at a site. The expected value and variance operators are applied over all the sites within a given station classification. We repeat these calculations for each scale and threshold combination. Figure 1 shows a plot of the mean residuals for each group against spatial scales for the 20 m threshold case. With the exception of PGA, sites that are classed in the high-lying group have positive residuals, sites that are classed in the low-lying group have negative residuals and neutral sites have nearly zero residuals. No trends are observed for PGA. We also analyze the single-station within-event standard deviation for each group (ϕ_{ss}) which is given by:

$$\phi_{ss}^2 = E(\phi_{ss,s}^2) \quad (5.2)$$

Figure 2 shows a plot of ϕ_{ss} against spatial scales for the 20 m threshold case. On average, neutral sites have lower ϕ_{ss} than high- or low-lying sites.

3.2 Advanced terrain-based classification (Iwahashi and Pike 2007)

Although the Iwahashi and Pike (2007) approach provided options for output classes of eight or 12 categories, we follow the approach of Yong *et al.* (2012) and investigate the maximum set of 16 terrain classes. Based on the co-locations of station sites and terrain types, we find all station sites to be located within only 15 of the 16 maximum terrain classes (Table 3.1). This outcome, however, is somewhat consistent with the findings of Yong *et al.* (2012) given no station sites were found to be associated with areas identified as terrain category of class 13 fitting the description of incised terraces. As to be expected, seismic monitoring sites generally tend to be located in major urban/metropolitan areas that are typically situated on soft basin-type terrains. The lesser number of seismic monitoring sites at hard rock locations—typically associated with mountainous or hilly sites—is expected to have a bearing on our analysis and will be discussed in a subsequent section.

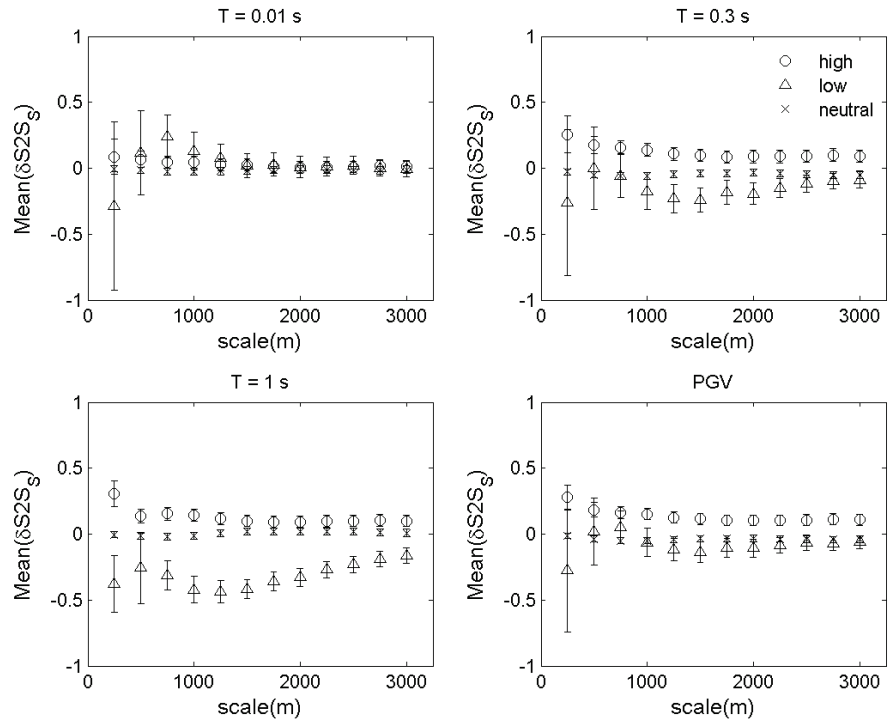


Figure 1. Mean $\delta S2S$ vs. spatial scale for the 20 m threshold. Vertical bars indicate the range for one standard-error of the mean estimate.

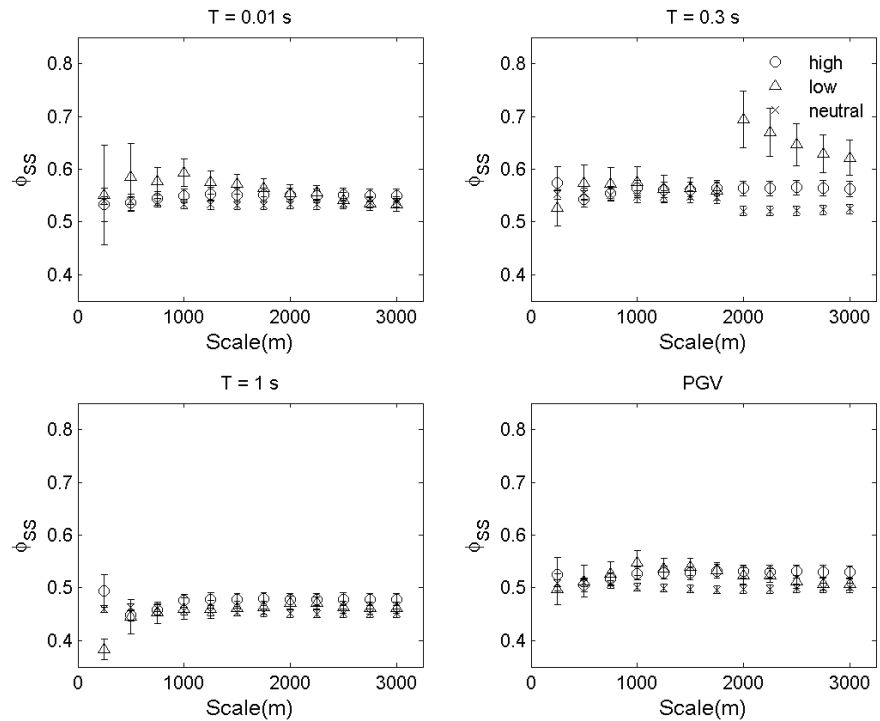


Figure 2. ϕ_{ss} vs. spatial scale for the 20 m threshold. Vertical bars indicate the range for one standard-error of the mean estimate.

Table 3.1. Terrain class and landform description (Iwahashi and Pike 2007).

Terrain class	Landform description	Number of stations
1	Well dissected alpine summits, mountains etc.	48
2	Large volcano, high block plateaus, etc.	1
3	Well dissected low mountains etc.	76
4	Volcanic fan, foot slope of high block plateaus etc.	71
5	Dissected plateaus, etc.	17
6	Basalt lava plain, glaciated plateaus, etc.	2
7	Moderately eroded mountains, lava flow, etc.	55
8	Desert alluvial slope, volcanic fan etc.	59
9	Well eroded plain of weak rocks, etc.	5
10	Valley, till plains, etc.	3
11	Eroded plain of weak rocks, etc.	25
12	Desert plain, delta plain, etc.	13
13	Incised terrace, etc.	0
14	Eroded alluvial fan, till plain, etc.	2
15	Dune, incised terrace, etc.	7
16	Fluvial plain, alluvial plain, low lying flat planes, etc.	28

In this assessment, mean $\delta S2S_S$, ϕ and ϕ_{ss} are calculated for each of the 15 categories. To expand our investigation, multiple terrain classes are aggregated to create super classes. In accordance to Yong *et al.* (2008), terrain types 1-4 are combined to form a super-class corresponding to mountains, terrain types 5-8 into a super-class called alluvial fans (piedmonts) and terrain types 9-16 into a set called basins/plains. Mean $\delta S2S_S$, ϕ and ϕ_{ss} are also calculated for each super set.

3.3 Analysis of variance (ANOVA)

Analysis of variance (ANOVA) is a statistical procedure for analyzing variance by partitioning the variable into components, each pertaining to a source of error. Principally, ANOVA provides a statistical test of whether or not the means of several groups are equal. Thus, generalizes the t-test to more than two groups. In this paper, we perform both one-way and two-way ANOVA using the R statistical software (R Development Core Team 2010) to check whether the mean $\delta S2S_S$ of the groups differ significantly. The implementation of this test is described below.

Case 1: One-Way ANOVA

We model the residual as $r_{ij} = \mu + \alpha_i + \epsilon_{ij}$ where r_{ij} is the residual for a site belonging to topographic group i at station j . We want to test if the effect of topography is significant or not. So the null hypothesis is:

$$H_0: \alpha_1 = \alpha_2 = \alpha_3$$

where the subscripts refer to topographic group. If the null hypothesis is rejected at a chosen significance level (95% for our exercise, which is equivalent to a p-value of 5% in the ANOVA test); we cannot assume the effect from topography to be insignificant. In order to test our assumption, we use one-way ANOVA for S_a at periods of $T = 0.01$ s, $T = 0.3$ s, $T = 1$ s and PGV.

Case 2: Two-Way ANOVA

In this case, we include any residual site effects which may not be captured by the parameters used in the ground motion prediction model. Hence, the residuals are modeled as:

$$r_{ijk} = \mu + \alpha_i + \beta_j + \epsilon_{ijk}$$

Here the residual (r_{ijk}) for a topographic class i , station j and recording k is modeled as an overall bias (μ) plus the effect of topography for group i (α_i) plus the repeatable site effects for site j (β_j) plus an unexplained residual (ϵ_{ijk}). We want to check if the effect of topography is significant, hence the null hypothesis again is:

$$H_0: \alpha_1 = \alpha_2 = \alpha_3$$

And if the null hypothesis is rejected, again for a p-value less than 0.05, we cannot assume the effect from topography to be insignificant.

4. RESULTS

Our analysis using the elevation-based classification method indicates a consistent bias in residuals for high-lying and low-lying stations. Both one-way and two-way ANOVA analyses indicate that the means for the three classes (high-lying, low-lying and neutral) are significantly different at most scales, thresholds, and periods; the only exception being at PGA for thresholds of 20m and 25m, for scales between 1750m and 2750m

For example, at the threshold of 20 m, the mean $\delta S2S_S$ for high-lying sites seem to be consistently greater than neutral-lying locations at all scales for S_a at $T = 0.3s$, $1s$ and PGV (Fig. 1). Also, the mean $\delta S2S_S$ for low-lying sites are lesser than that for high- and neutral-lying locations. These differences are observed to be most prominent at the longer period ($T = 1 s$) which have been previously attributed by Ødegaard *et al.* (1990) as an indication of topography-induced site response. In Figure 2, for the same threshold, ϕ_{ss} is observed to be typically greater for low- and high-lying sites and lesser for neutral locations at most scales. Because neutral-lying sites have lower ϕ_{ss} than sites that are high- or low-lying, the expected ground motion variability recorded at a site can be expected to be smaller if the site belongs to the neutral-lying class. However, the trends in the ϕ_{ss} values (Fig. 2) for each ground motion parameter do not appear to be as stable as the trends observed for the mean $\delta S2S_S$ relations to each spatial scale (Fig. 1). Figure 3 also shows similar trends, where ϕ values are usually greater for high- and low-lying sites and lesser for the neutral locations at most scales. Similar trends are also observed for other thresholds (not shown).

At a scale of 1250 m and threshold of 20 m, high-lying stations are observed to have the largest mean $\delta S2S_S$ amongst the three classes and low-lying stations are observed to have the smallest mean $\delta S2S_S$ for almost all ground motion parameters—the neutral sites mostly appear to lie somewhere in between (Fig. 4 and Table 4.1). Consistent with earlier observations, ϕ_{ss} is greater for high-lying and low-lying sites and lesser for the neutral locations.

Table 4.1. Mean $\delta S2S$ and ϕ_{ss} for the elevation-based scheme at a scale of 1250 m and a threshold of 20 m

	Mean($\delta S2S$)				ϕ_{ss}			
	$T = 0.01s$	$T = 0.3s$	$T = 1s$	PGV	$T = 0.01s$	$T = 0.3s$	$T = 1s$	PGV
High-lying	0.0274	0.1075	0.1159	0.1246	0.5524	0.5614	0.4783	0.5289
Low-lying	0.0806	-0.2291	-0.4375	-0.1184	0.5748	0.5627	0.4592	0.5370
Neutral	-0.0217	-0.0440	0.0054	-0.0410	0.5324	0.5484	0.4543	0.4993

In our evaluation of the Iwahashi and Pike (2007) classification scheme, we investigate mean $\delta S2S_S$ for each individual terrain class and for a combination of different classes, e.g. super classes consisting of mountains, alluvial fans and basins/plains. Our preliminary results indicate no obvious relations between mean $\delta S2S_S$ and individual or the aggregated classes of terrain. However, we note that the averaging of effects over different classes may have a significant influence on the low mean $\delta S2S_S$ values for the features shown in Table 4.2. To explore this and other possibilities, we intend to fully

investigate the utility of the terrain classification method as well as other classification techniques in future studies.

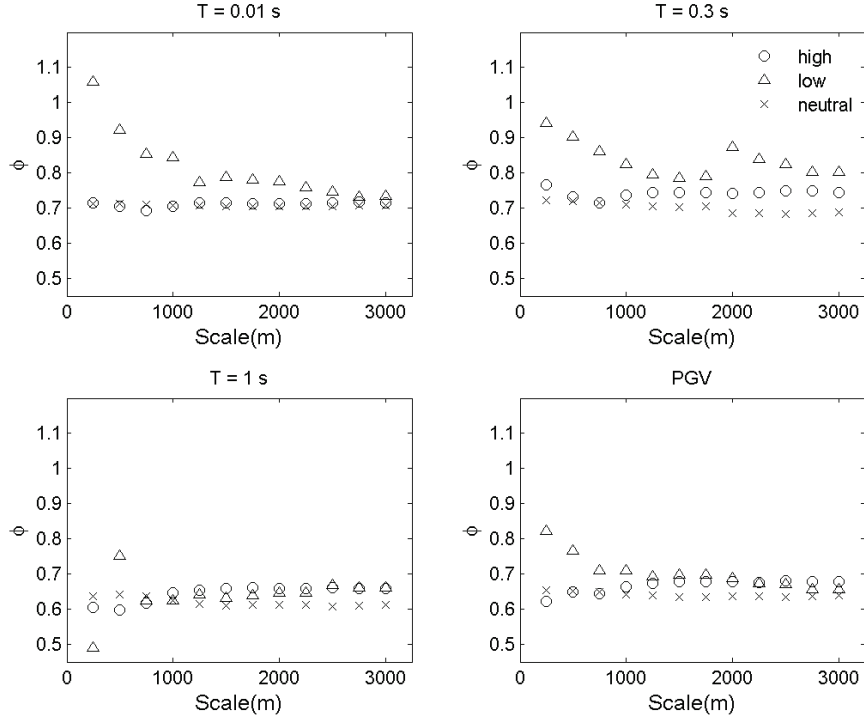


Figure 3: ϕ vs. spatial scale for a 20 m threshold.

Table 4.2. Mean $\delta S2S$ for three super classes from Iwashashi and Pike's (2007) classification

Class	Super class	Feature	Mean $\delta S2S_g$			
			T = 0.01 s	T = 0.3 s	T = 1 s	PGV
1 - 4	1	Hill	0.00427	-0.02522	-0.04843	0.01319
5 - 8	2	Alluvial Fans	-0.01586	-0.00903	0.04174	-0.00798
9 - 16	3	Basins/Plains	0.00049	-0.02023	0.06461	-0.04542

5. DISCUSSION

The results from the previous section indicate that the elevation-based classification scheme is capable of discriminating three station classes (high-, low-, and neutral-lying) each with distinct trends in the intra-event residuals. Given these residuals were computed with respect to a GMPE (Chiou *et al.*, 2010) that considered site response using V_{S30} , site effects should have, in principle, been accounted for. Therefore, it is tempting to assume that the observed trends in the residuals are directly attributable to topographic effects; however, it is also likely that a significant part of these observations are a result of known shortcomings when using V_{S30} for parameterizing site response (Anderson *et al.*, 1996; Wald and Mori, 2000; Castellaro *et al.*, 2008). For example, relative elevation, as introduced in this paper, can potentially explain residuals from one-dimensional site effects that are not captured by V_{S30} . Moreover, much of the V_{S30} values associated with the stations in the SMM earthquake database were obtained by correlations with surface geology and hence cannot be assumed to be completely reliable (Yong *et al.*, 2012). Finally, relative elevation may also have the potential to act as a proxy for effects not yet understood.

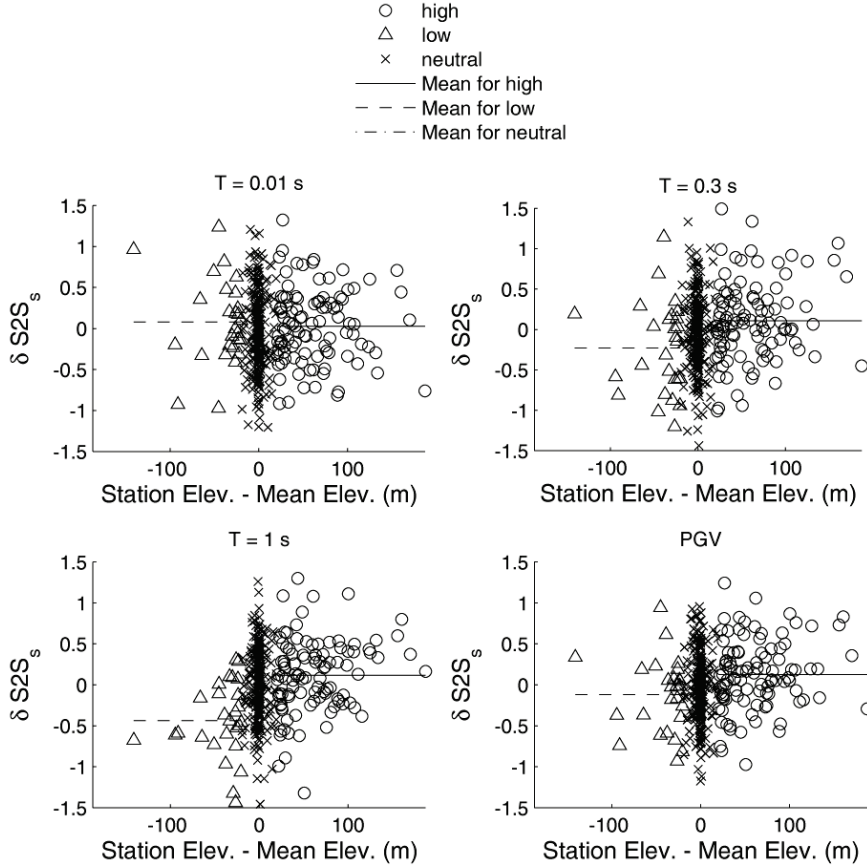


Figure 4. Plot of mean intra-event station residuals (δS_{2S}) as a function of relative elevation for a spatial scale of 1250 m and a threshold of 20 m. The lines represent the mean residuals for each class (high-, low- and neutral-lying).

Despite these observations, it is clear that using relative elevation can lead to a reduction in the bias of estimates from the GMPE based on the SMM earthquake database. This reduction is demonstrated to be significant (Fig. 1). Moreover, the larger values of ϕ_{ss} at stations in high- or low-lying locations can also be brought to bear on the results of site-specific seismic hazard analyses. Additional studies are needed to confirm the link between relative elevation and topographic effects. Current work is being conducted to repeat these analyses for a larger database including large magnitude earthquakes, and for databases in different geographical locations (e.g., Japan and Taiwan).

6. SUMMARY AND CONCLUSIONS

In this study we investigate the residuals of the California Small and Medium Magnitude database to study the effect of surface topography on the ground motion residuals. We evaluate two classification schemes, both of which are computed directly from elevation data. Results indicate that there is a statistically significant bias on the residuals for different topography classes. These parameterizations can be included in future GMPE development to improve prediction of strong ground motions.

ACKNOWLEDGEMENT

This material is based on work supported by the National Science Foundation under Grant No. CMMI-1132373. Any opinions, findings and conclusions or recommendations expressed in this material are those of the authors and do not necessarily reflect the views of the National Science Foundation. We are indebted to the National Research Institute for Earth Science and Disaster Prevention (NIED) in Japan for providing the data for this analysis.

REFERENCES

- Al Atik, L., Abrahamson, N., Cotton, F., Scherbaum, F., Bommer, J.J. and Kuehn, N.M. (2010). The variability of ground-motion prediction models and its components, *Seismological Research Letters*, **81** (5), 794–801.
- Anderson, J. G., Lee, Y., Zeng, Y. and Day, S. (1996). Control of strong motion by the upper 30 meters, *Bulletin Seismological Society of America*, **86** (6), 1749-1759.
- Assimaki, D., and Gazetas, G. (2004). Soil and topographic amplification on canyon banks and the 1999 Athens earthquake, *Journal of Earthquake Engineering*, **8** (1), 1-43.
- Bard, P-Y. (1982). Diffracted waves and displacement field over two-dimensional elevated topographies, *Geophysical Journal of the Royal Astronomical Society*, **71**, 731-760.
- Benjamin, J. R. and Cornell, C. A. (1970). Probability, statistics, and decision for civil engineers, McGraw-Hill, New York.
- Boore, D. M., Harmsen, S. C. and Harding, S.T. (1981). Wave scattering from a step change in surface topography, *Bulletin Seismological Society of America*, **71** (1), 117-125.
- Bouchon, M., (1973). Effect of topography on surface motion, *Bulletin Seismological Society of America*, **63** (3), 615-632.
- Castellaro, S., Mulargia, F. and Rossi, P. L. (2008). Vs30: proxy for seismic amplification?, *Seismological Research Letters*, **79** (4), 540-543.
- Çelebi, M. (1991), Topographical and geological amplification: case studies and engineering implications, *Structural Safety*, **10**, 199-217.
- Chiou, B., Youngs, R., Abrahamson, N. and K. Addo (2010).Ground-Motion attenuation model for small-to-moderate shallow crustal earthquakes in California and its implications on regionalization of ground-motion prediction models, *Earthquake Spectra*, **26** (4), 907-926.
- Dikau, R., Brabb, E. E. and Mark, R. M. (1991). Landform classification of New Mexico by computer, *U. S. Geological Survey Open-File Report*, 91-634, 1-15.
- Geli, L., Bard, P-Y. and Jullien, B. (1988). The effect of topography on earthquake ground motion: a review and new results, *Bulletin Seismological Society of America*, **78** (1), 42-63.
- Grazier, V. (2009). Low-velocity zone and topography as a source of site amplification effect on Tarzana hill, California, *Soil Dynamics and Earthquake Engineering*, **29**, 324-332.
- Hough, S. E., Yong, A., Altidor, J. R., Anglade, D., Given, D. and Mildor, S-L. (2011). Site characterization and site response in Port-au-Prince, Haiti, *Earthquake Spectra*, **27** (S1), S137-S155.
- Iwashashi, J. and Pike, R. J. (2007). Automated classifications of topography from DEMs by an unsupervised nested-means algorithm and a three-part geometric signature, *Geomorphology*, **86**, 409-440.
- Miliaresis, G. Ch. and Argalias, D.P. (1999). Segmentation of physiographic features from the global digital elevation model/GTOPO30, *Computers and Geosciences*, **25**, 715-728.
- Ødegaard, E. and Doornbos, D. J. and Kværna, T. (1990). Surface topographic effects at arrays and three-component stations, *Bulletin of the Seismological Society of America*, **80**(6B), 2214-2226
- R Development Core Team (2010). R: A Language and Environment for Statistical Computing, R Foundation for Statistical Computing Vienna Austria 2010 {ISBN} 3-900051-07-0, URL <http://www.R-project.org>.
- Sánchez-Sesma, F. J. (1983). Diffraction of elastic waves by three-dimensional surface irregularities, *Bulletin Seismological Society of America*, **73** (6), 1621-1636.
- Schmidt, J. and Hewitt, A. (2004). Fuzzy land element classification from DTMs based on geometry and terrain position, *Geoderma*, **121**, 243-256.
- Shakal, A., Huang, M., Darragh, R., Cao, T., Sherburne, R., Malhotra, P., Cramer, C., Sydnor, R., Graizer, V., Maldonado, G., Peterson, C. and Wampole, J. (1994). CSMIP Strong motion records from the Northridge, California, earthquake of 17 January 1994, Report OSMS 94-07, Calif. Div. Mines Geol., Sacramento, California.
- Spudich, P., Hellweg, M. and Lee, W. H. K. (1996). Directional topographic site response at Tarzana observed in aftershocks of the 1994 Northridge, California, earthquake: implications for mainshock motions, *Bulletin Seismological Society of America*, **86** (1B), S193-S208.
- Wald, L. A. and Mori, J. (2000). Evaluation of methods for estimating linear site-response amplifications in the Los Angeles region, *Bulletin of the Seismological Society of America*, **90** (6B), S32-S42.
- Wood, J. (1996). The Geomorphological Characterisation of Digital Elevation Models, PhD Thesis, Department of Geography, University of Lancaster, UK.
- Yong, A., Hough, S. E., Iwashashi, J. and Braverman, A. (2012). A Terrain-based site-conditions map of California with implications for the contiguous United States, *Bulletin of the Seismological Society of America*, **102** (1), 114-128.